

# Sustained calcium signalling and caspase-3 activation involve NMDA receptors in thymocytes in contact with dendritic cells

P Affaticati<sup>1,2,3</sup>, O Mignen<sup>1,2,3</sup>, F Jambou<sup>1,2,3</sup>, M-C Potier<sup>4</sup>, I Klingel-Schmitt<sup>1,2,3,12</sup>, J Degrouard<sup>5</sup>, S Peineau<sup>6,7</sup>, E Gouadon<sup>1,2,3,12</sup>, GL Collingridge<sup>6,8,9</sup>, R Liblau<sup>10</sup>, T Capiod<sup>11</sup> and S Cohen-Kaminsky<sup>\*,1,2,3,12</sup>

L-glutamate, the major excitatory neurotransmitter, also has a role in non-neuronal tissues and modulates immune responses. Whether NMDA receptor (NMDAR) signalling is involved in T-cell development is unknown. In this study, we show that mouse thymocytes expressed an array of glutamate receptors, including NMDARs subunits. Sustained calcium ( $\text{Ca}^{2+}$ ) signals and caspase-3 activation in thymocytes were induced by interaction with antigen-pulsed dendritic cells (DCs) and were inhibited by NMDAR antagonists MK801 and memantine. NMDARs were transiently activated, triggered the sustained  $\text{Ca}^{2+}$  signal and were corecruited with the PDZ-domain adaptor postsynaptic density (PSD)-95 to thymocyte-DC contact zones. Although T-cell receptor (TCR) activation was sufficient for relocalization of NMDAR and PSD-95 at the contact zone, NMDAR could be activated only in a synaptic context. In these T-DC contacts, thymocyte activation occurred in the absence of exogenous glutamate, indicating that DCs could be a physiological source of glutamate. DCs expressed glutamate, glutamate-specific vesicular glutamate transporters and were capable of fast glutamate release through a  $\text{Ca}^{2+}$ -dependent mechanism. We suggest that glutamate released by DCs could elicit focal responses through NMDAR-signalling in T cells undergoing apoptosis. Thus, synapses between T and DCs could provide a functional platform for coupling TCR activation and NMDAR signalling, which might reflect on T-cell development and modulation of the immune response.

*Cell Death and Differentiation* (2011) 18, 99–108; doi:10.1038/cdd.2010.79; published online 25 June 2010

L-glutamate is the major excitatory neurotransmitter in the central nervous system (CNS). There is now evidence to suggest that glutamate acts as a signalling molecule in non-neuronal tissues,<sup>1,2</sup> with an emerging role as an immune modulator.<sup>3</sup> Metabotropic G-protein-coupled glutamate receptors (mGluRs) are involved in T-cell activation,<sup>4</sup> and in the inhibition of activation-induced cell death.<sup>5</sup> Ionotropic glutamate receptors are involved in cell cycle progression, regulating activation and proliferation, chemotactic migration and integrin-mediated adhesion in T cells,<sup>6,7</sup> with some indications for a role of the *N*-methyl-D-aspartate receptor (NMDAR) in  $\text{Ca}^{2+}$  signalling.<sup>8,9</sup>

Increases in  $[\text{Ca}^{2+}]_i$  are key signals in T-cell activation after T-cell receptor (TCR) engagement. T lymphocytes are believed to use store-operated calcium (SOC) channel entry

as the main mode of  $\text{Ca}^{2+}$  influx.<sup>10</sup> The SOC channels in lymphocytes are known as  $\text{Ca}^{2+}$  release-activated  $\text{Ca}^{2+}$  (CRAC) channels, whose molecular identity has been recently elucidated, with Orai1 as the pore-forming subunit and STIM1 as the sensor of stored  $\text{Ca}^{2+}$ .  $\text{Ca}^{2+}$  signalling in T cells also involves purinergic receptors, voltage-gated  $\text{Ca}^{2+}$  channels, and activate other channels such as  $\text{Ca}^{2+}$ -dependent voltage-activated  $\text{K}^+$  channels.<sup>11,12</sup> The relationships between all these  $\text{Ca}^{2+}$  routes, remain to be elucidated.

The immunological synapse (IS) is a structure that mediates information exchange, which forms in the contact zone between an antigen-presenting cell (APC) and a T-cell bearing a specific TCR. It was first suggested to facilitate the directed secretion of cytokines between T cells and APCs.<sup>13</sup>

<sup>1</sup>Centre National de la Recherche Scientifique (CNRS), Département des Sciences du Vivant (DSV), Institut National des Sciences Biologiques (INSB), Unité Mixte de Recherche UMR 8162, Institut Paris Sud Cytokines, Le Plessis Robinson, Ile de France F-92350, France; <sup>2</sup>Univ. Paris-Sud, Orsay F-91405, Faculté de Médecine Paris-Sud, Le Kremlin-Bicêtre F-94270, France; <sup>3</sup>Hôpital Marie Lannelongue, Département de Recherche Médicale, Le Plessis-Robinson F-92350, France; <sup>4</sup>Centre National de la Recherche Scientifique (CNRS), Unité Mixte de Recherche UMR 7637, Département de Neurobiologie et Diversité Cellulaire, ESPCI, Paris F-75005, France; <sup>5</sup>Centre National de la Recherche Scientifique (CNRS), Unité Mixte de Recherche UMR 8080, Département de Microscopie Electronique, Université Paris-Sud, Orsay F-91405, France; <sup>6</sup>Department of Anatomy, MRC Centre for Synaptic Plasticity, School of Medical Sciences, Bristol, UK; <sup>7</sup>Institut National de la Recherche Médicale, INSERM, U676, Département de physiopathologie et neuroprotection des atteintes du cerveau en développement, Hôpital Robert Debré, Université Paris 7, Faculté de Médecine Denis Diderot Paris, Paris F-75019, France; <sup>8</sup>Department of Psychiatry, Brain Research Centre, University of British Columbia, Vancouver, British Columbia V6T-1Z3, Canada; <sup>9</sup>Department of Brain and Cognitive Sciences, Seoul National University, Seoul 151747, Korea; <sup>10</sup>Institut National de la Santé et de la Recherche Médicale, INSERM U563, Département d'Immunologie et Maladies Infectieuses, Hôpital Universitaire Purpan, Toulouse, F-31000, France; <sup>11</sup>Institut National de la Santé et de la Recherche Médicale, INSERM, U1003, IFR147, Université Lille 1, Villeneuve d'Ascq F-59655, France and <sup>12</sup>Institut National de la Recherche Médicale, INSERM U999, Institut d'Immunologie, Hématologie, Pneumologie, Le Plessis Robinson F-92350, France

\*Corresponding author: S Cohen-Kaminsky, INSERM U999, Université Paris Sud, Hôpital Marie Lannelongue, 133 Avenue de la Résistance, F-92350, Le Plessis-Robinson, France. Tel: +33 1 40 94 25 14; Fax: +33 1 40 94 25 22; E-mail: sylvia.cohen-kaminsky@u-psud.fr

**Keywords:** calcium signalling; thymocyte; NMDAR; glutamate signalling; immunological synapse

**Abbreviations:** APC, antigen-presenting cell;  $\text{Ca}^{2+}$ , calcium; CRAC,  $\text{Ca}^{2+}$  release-activated  $\text{Ca}^{2+}$ ; CNS, central nervous system; DC, dendritic cell; DP,  $\text{CD4}^+\text{CD8}^+$  double-positive; GluR, glutamate receptor; IS, immunological synapse; mGluR, metabotropic glutamate receptor; NMDA, *N*-methyl-D-aspartate; NMDAR, NMDA receptor; PSD, postsynaptic density; SOC, store-operated calcium channel; TCR, T-cell receptor; VGLUT, vesicular glutamate transporter

Received 13.11.09; revised 27.4.10; accepted 17.5.10; Edited by A Verkhatsky; published online 25.6.10

Cytokines may be released into the synapse, having an immediate effect on clustered receptors in the contact zone.<sup>14</sup> The synapse formed between T cells and dendritic cells (DCs) shows cell-to-cell adhesion, stability and close apposition of membranes,<sup>15</sup> which may help to optimize soluble mediator concentration at the T cell-APC interface, thereby limiting bystander effects. Neuronal synapses and ISs show anatomical similarity, although ISs form rapidly and are transient.<sup>16</sup> To what extent these synapses are functionally similar is not known.

Circulating T cells are thought to be exposed to glutamate in the plasma, glutamate-rich peripheral organs,<sup>1,2</sup> and in the brain, facilitating cross-talk with the CNS.<sup>17</sup> It is therefore likely that GluRs are not permanently stimulated in T cells, and we postulated that their activation occurs as a result of IS formation. In analogy to neurons, glutamate should therefore be rapidly released, with faster kinetics than those reported through the cystine/glutamate antiporter ( $X_c^-$  system).<sup>18</sup> Indeed, the possibility that glutamate released by APCs at ISs mediates communication with T cells through GluR-mediated  $Ca^{2+}$  signalling has never been analyzed.

As glutamate mediates apoptosis of neuronal cells through NMDARs and  $Ca^{2+}$  signalling,<sup>19</sup> we analyzed thymocyte development, a process in which thymocytes that recognize self-antigens with high affinity are eliminated by  $Ca^{2+}$ -dependent apoptosis.<sup>20</sup> Our findings indicate that DCs

are capable of fast  $Ca^{2+}$ -dependent glutamate release, while thymocytes express NMDARs, which modulate TCR-dependent  $Ca^{2+}$  signalling and apoptosis only in a synaptic context, revealing a novel aspect of IS functioning.

## Results

**NMDARs are expressed in thymocytes.** More than 30 different GluRs are expressed in the CNS.<sup>21</sup> As only mGluRs have been detected in thymocytes,<sup>22</sup> we used neurotransmission-dedicated oligoarrays to analyze their GluR repertoire. Thymocytes expressed most known GluRs (Supplementary Figure S1a), including NMDAR GluN1, GluN2A and GluN2B subunits (IUPHAR nomenclature of subunits), previously referred to as NR1, NR2A and NR2B subunits<sup>23</sup> (Figure 1a). These findings were confirmed by PCR (Figure 1a), and confocal microscopy, using well-characterized antibodies (Figure 1b, Supplementary Figure S1c). To study NMDAR function, we focused on NR1, the obligate subunit of NMDARs, which was expressed in thymocytes at levels similar to what was observed in the brain (Figure 1a, Supplementary Table S1). FACS analysis, indicated that 97.3% of thymocytes expressed NR1, with higher expression in  $CD4^+$  or  $CD8^+$  cells as compared with  $CD4^+CD8^+$  double-positive (DP) cells (Figure 1c).

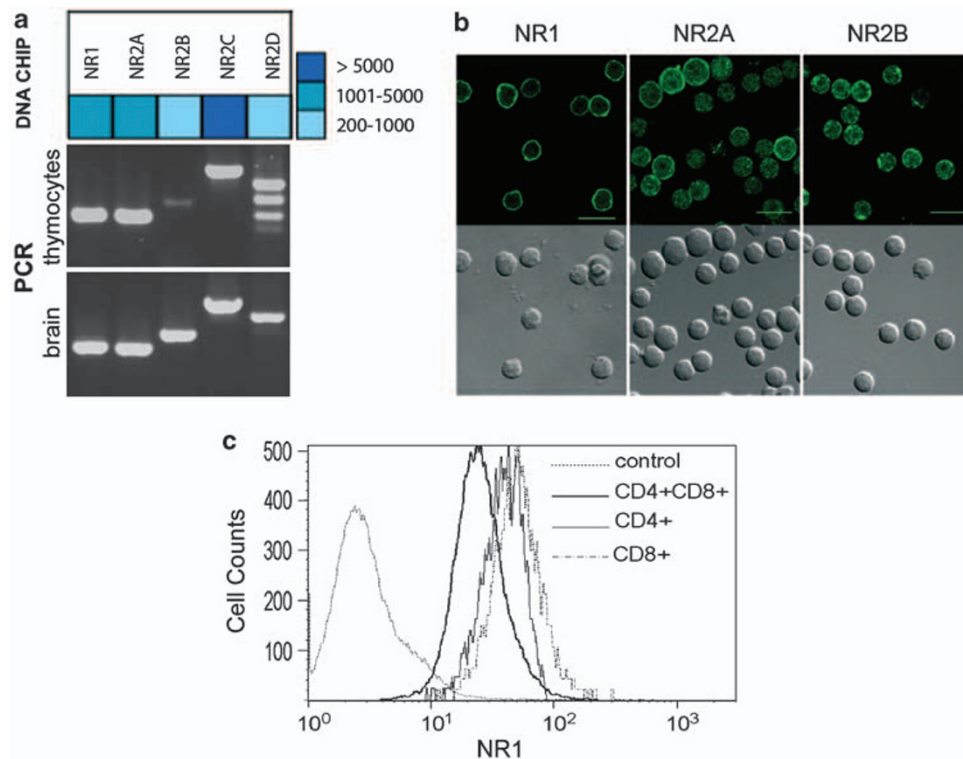


**Figure 1** T cells express a large array of i- and m-GluRs. (a) Oligoarray (Neurotrans) analysis of NMDAR mRNA expression on thymocytes compared with brain (upper panel), and validated by RT-PCR compared with brain (lower panel). Oligoarray data are shown as a heat map. Data for all GluRs are shown in Supplementary Figure S1 using primers shown in Supplementary Table S1. (b) Immunofluorescence analysis of NMDAR subunit expression on thymocytes. For each indicated NMDAR subunit (NR1, NR2A, NR2B), a Nomarski image (bottom row) and a confocal fluorescence image is shown in an equatorial plane (top row). Images for other ionotropic glutamate receptors (iGluRs) are shown in Supplementary Figure S1c. Control staining consisting in IgG2b isotype control (for anti-NR1 antibody) or purified rabbit IgG (for anti-NR2A, NR2B, GluR2/3, KA2 antibodies) were negative using the same settings as the specific staining (Supplementary Figure S1c). (c) Flow cytometry analysis of NR1 expression in thymocytes. Antibodies that detect NR1 as a band at the expected molecular weight by western blotting in brain microsomal preparations were used. Relative fluorescence intensity is shown for  $CD4^+$ ,  $CD8^+$  and DP subpopulations. Data are representative of three independent experiments. IgG2b control isotype is shown as control for NR1 staining

**Ca<sup>2+</sup> signalling and apoptosis in thymocytes in contact with DCs, involves NMDAR.** To examine NMDAR function in thymocytes, we focused on Ca<sup>2+</sup> and apoptosis signalling. Indeed, both are associated with NMDAR activity in neurones. Glutamate and NMDA, at doses of 1–500  $\mu$ M, did not induce Ca<sup>2+</sup> signalling or apoptosis in thymocytes (data not shown). Thus, we analyzed whether a thymocyte-DC synaptic context could provide the environment required for coupling Ca<sup>2+</sup> signalling to apoptosis.

To set up an *in vitro* system of T cell-DC synapses, we used HNT-TCR-transgenic mice in which most T cells express the same TCR directed to the HA 126–138 peptide. *In vivo* administration of HA 126–138 in transgenic mice induces massive apoptosis, mostly of DP thymocytes.<sup>24</sup> Coculture of thymocytes from transgenic mice and HA-pulsed DCs, enhances the probability of antigen-dependent synaptic contacts. To assess DC capacity to induce thymocyte apoptosis, we monitored the expression of Nur77, CD69 and caspase-3. Nur77, an immediate early gene required for the induction of apoptosis in negative selection<sup>25</sup> is a specific marker of clonal deletion *in vivo*.<sup>26</sup> CD69, an early T-cell activation marker upregulated after TCR engagement and involved in negative selection,<sup>27</sup> was thus used to discriminate thymocytes that have contacted DCs. Activated caspase-3 in living cells, allowed early detection of apoptosis, avoiding bystander effects occurring at later time points. Nur77, CD69 and activated caspase-3 that we measured *in vivo*, were also upregulated *in vitro*, indicating functional synapses *in vitro* (Supplementary Figure S2a). In contrast to thymocytes, peripheral CD4<sup>+</sup> T cells in contact with DCs showed increased CD69 expression, without caspase-3 activation (Supplementary Figure S2b) and proliferated as expected in response to HA peptide (data not shown).

Then, we used this *in vitro* system to monitor the Ca<sup>2+</sup> signal elicited in thymocytes contacting DCs. Antigen-specific contacts of thymocytes with DCs, in a glutamate-free medium, resulted in rapid and sustained increase in [Ca<sup>2+</sup>]<sub>i</sub> in T cells (Figures 2a and b). A majority of the thymocytes established long-lasting contacts, 90% of which resulted in a Ca<sup>2+</sup> peak ( $\Delta R/R = 2.93 \pm 0.08$ ,  $n = 119$ ), followed by a sustained high-level plateau lasting at least 10 min (Figure 2b and Supplementary Video S1). A few unstable contacts with no measurable Ca<sup>2+</sup> signals were observed in the absence of HA-peptide (Figure 2b). Interestingly, contacts with peripheral splenic CD4<sup>+</sup> T cells resulted in a Ca<sup>2+</sup> signal with a peak similar to that for thymocytes ( $\Delta R/R = 3.72 \pm 0.19$ ,  $n = 32$ ), but rapidly decreasing (50% decrease from the peak value in  $91 \pm 13$  s,  $n = 30$ ) to a plateau maintained at a basal level of approximately one-fifth of the peak value (Figures 2a and c, Supplementary Videos S1 and S2).

Thus, thymocyte-DC contact, in the absence of exogenous glutamate, results in a sustained Ca<sup>2+</sup> signal with a high plateau and apoptosis signalling. These results also point to a potential relationship between the sustained shape of the Ca<sup>2+</sup> signal and T-cell fate.

**NMDAR triggers the sustained Ca<sup>2+</sup> response in thymocytes and is involved in thymocyte apoptosis.** The primary mechanism of Ca<sup>2+</sup> mobilization in T cells is the release of Ca<sup>2+</sup> from intracellular stores

followed by Ca<sup>2+</sup> influx through CRAC channels.<sup>10</sup> We hypothesized that NMDARs could participate in Ca<sup>2+</sup> influx, thereby contributing to the sustained Ca<sup>2+</sup> plateau observed during thymocyte apoptosis.

In the T-DC synapse model, we incubated T cells either with MK801 or memantine, two non-competitive open-channel NMDAR blockers, and then measured T-DC contact-induced Ca<sup>2+</sup> signals and apoptosis in presence of these inhibitors. MK801 and memantine modulated Ca<sup>2+</sup> signals in approximately 50% of thymocytes, resulting in a transient signal with a similar amplitude at the initial peak ( $3.15 \pm 0.14$ ,  $n = 42$  and  $2.81 \pm 0.12$ ,  $n = 33$ , for MK801 and memantine, respectively) to control cells, but with a plateau close to basal levels (50% decrease in the peak value after  $148 \pm 16$  s,  $n = 18$  and  $275 \pm 37$  s,  $n = 14$ , respectively) (Figure 2d and Supplementary Video S3). To rule out the possibility that NMDAR blockers had non-specific effects on CRAC or other off-target effects on channels involved in T-cell activation, we monitored the Ca<sup>2+</sup> signal by FACS on thymocytes activated by anti-CD3/anti-CD28 cross-linking, in the absence of glutamate. Approximately 60% of thymocytes responded to TCR stimulation by a Ca<sup>2+</sup> signal that was unaffected by MK801 or memantine (Supplementary Figure S3), indicating that these drugs had no major effect on Ca<sup>2+</sup> signalling resulting from TCR triggering.

NMDAR blockers also significantly affected the percentages of activated caspase-3-expressing cells ( $27 \pm 0.7\%$  inhibition with MK801,  $n = 24$  and  $30 \pm 0.85\%$  with memantine,  $n = 15$ ) (Figure 3a), indicating a role for NMDARs in apoptosis. It is noteworthy that the effect on caspase-3 expression might be underestimated because only 50% of thymocytes engaged in a synapse were sensitive to the drugs, as measured in Ca<sup>2+</sup> signalling experiments. Activation of Nur77 expression, which is Ca<sup>2+</sup> dependent, was affected by MK801 as measured by FACS analysis, 4 h after thymocyte-DC contact (Figures 3b and c), suggesting that Nur77 could be an early target of the Ca<sup>2+</sup> signal mediated by NMDAR.

As previously mentioned glutamate or NMDA did not induce any Ca<sup>2+</sup> signalling, in freshly dissociated thymocytes. Patch-clamp recordings confirmed that no NMDA current was detectable, when NMDA and D-serine were co-applied (data not shown), indicating NMDA insensitivity of isolated thymocytes. These data, combined to the observation that NMDAR blockers inhibit both Ca<sup>2+</sup> and apoptosis signalling in DC-contacting thymocytes, suggest that NMDA channels are activated only during or after synapse formation. To further analyze the involvement of NMDA channels in this process, we asked if (1) NMDARs are activated only after synapse formation and (2) the sustained Ca<sup>2+</sup> response requires a transient NMDAR activation. Using the T-DC contact model, we incubated freshly dissociated thymocytes with MK801, NMDA and D-serine to block all activable NMDARs present at the membrane. We then washed the thymocytes and recorded the Ca<sup>2+</sup> signals after synaptic T-DC contact. The sustained Ca<sup>2+</sup> responses ( $n = 47$ , 95% of cells with a sustained signal) (Figure 3d), were similar to the responses recorded in absence of thymocyte pre-treatment, suggesting that NMDARs are active only after synaptic contact even if their agonists are present. In the



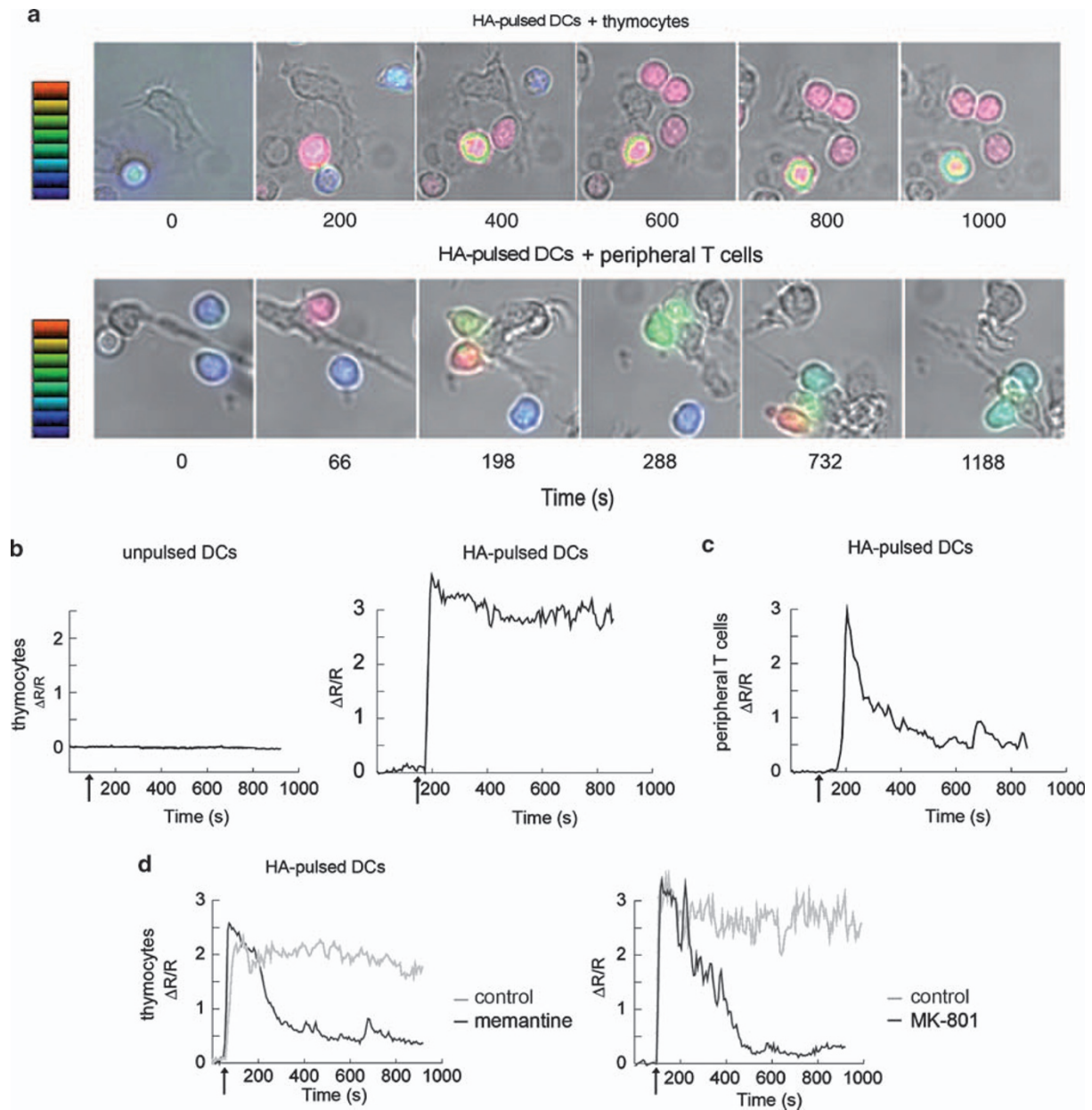


**Figure 2** NMDAR modulates  $\text{Ca}^{2+}$  signalling in thymocytes in contact with DCs, in the absence of exogenous glutamate. **(a)** Representative time-lapse microscopy images (DIC/Fura-2 overlay) of thymocytes (upper set) and peripheral T cells (lower set) making contact with HA-pulsed DCs. The scale indicates  $\text{Ca}^{2+}$  level, expressed as  $\Delta R/R$  values, ranging from 0 (blue) to 3 (red). In thymocytes, steep  $[\text{Ca}^{2+}]_i$  increases were recorded  $44 \pm 3$  s ( $n = 101$ ) after initial contact with the DC, and was, in most synapses, rapidly followed by the establishment of a stable contact ( $50 \pm 2$  s,  $n = 93$ ) associated with a sustained high-level plateau lasting at least 10 min. **(b)** Representative  $\text{Ca}^{2+}$  signal in Fura-2 loaded thymocytes in contact with unpulsed DCs (left panel) or with HA-pulsed DCs (right panel). Arrows: contact. **(c)** Representative  $\text{Ca}^{2+}$  signal in Fura-2 loaded peripheral T cells in contact with HA-pulsed DCs. Arrow: contact. **(d)** Representative traces of the  $\text{Ca}^{2+}$  response in thymocytes in contact with HA-pulsed DCs in the presence (black curves) or absence (grey curves) of the NMDAR antagonists memantine ( $100 \mu\text{M}$ ) (left panel) and MK801 ( $100 \mu\text{M}$ ) (right panel). Arrows: contact

same conditions of pretreatment, addition of MK801 in the bath solution before synapse formation revealed a sensitivity of the  $\text{Ca}^{2+}$  plateau to this NMDAR blocker ( $n = 22$ , 55% of cells with a transient signal) (Figure 3d). Using the same protocol, 200 s after the beginning of  $\text{Ca}^{2+}$  signalling because of T-DC contacts, we applied MK801. MK801 application after synapse formation failed to inhibit  $\text{Ca}^{2+}$

response ( $n = 20$ , 90% of cells with a sustained signal) (Figure 3e).

Together, these results suggest that NMDARs are necessary for the induction of the sustained  $\text{Ca}^{2+}$  response but are only transiently activated at the beginning of the synaptic response. Furthermore, these receptors are also involved in the induction of thymocyte apoptosis after contact with DCs.

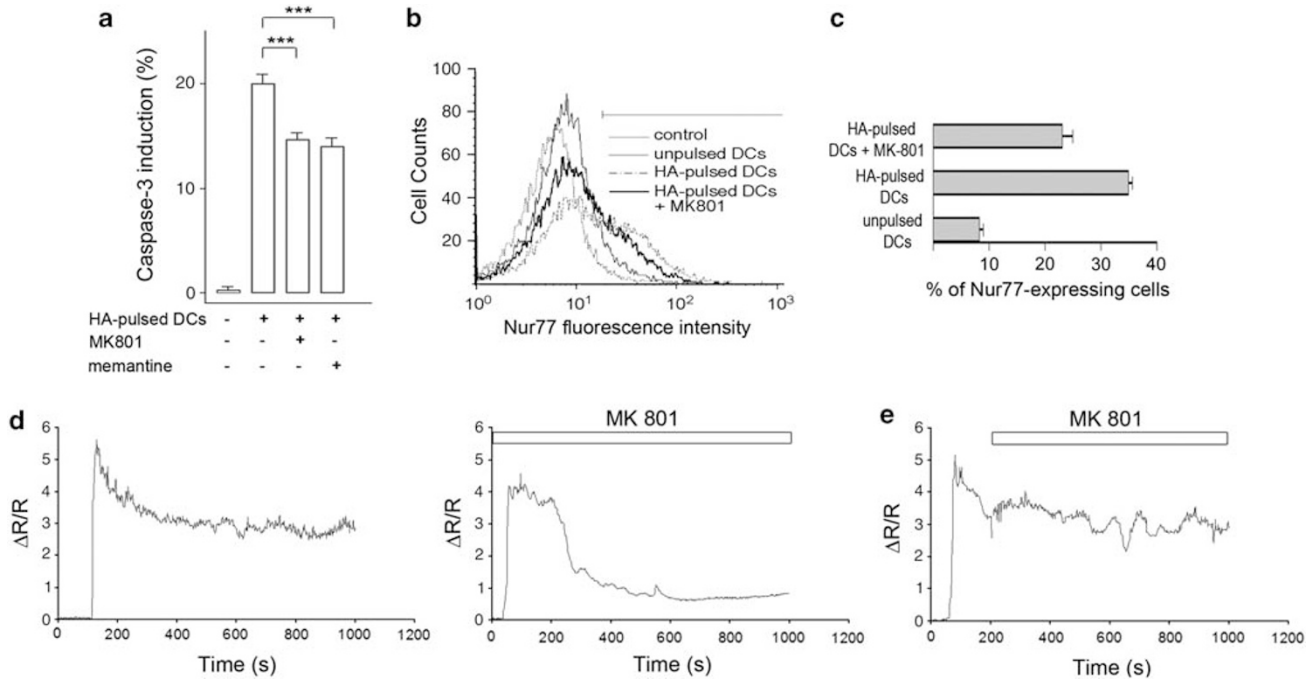


**Figure 3** NMDAR triggers a sustained  $\text{Ca}^{2+}$  signal, is transiently activated and is involved in caspase-3 activation and Nur77 induction, in thymocyte-DC contacts. (a) Inhibition of caspase-3 ( $t = 6$  h) expression in DP thymocytes co-cultured with unpulsed or HA-pulsed DCs with or without MK801 ( $100 \mu\text{M}$ ) and memantine ( $100 \mu\text{M}$ ). Data are means of six replicates for five independent cultures ( $*** P < 0.001$ ). The effect of memantine or MK801 on apoptosis was dose-dependent and was significant at  $10 \mu\text{M}$ , with the maximal effect observed at  $100 \mu\text{M}$ . A dose of  $10 \mu\text{M}$  MK801 resulted in  $11.4 \pm 1\%$  inhibition of apoptosis ( $n = 6$ ) and a transient  $\text{Ca}^{2+}$  signal in 50% thymocytes ( $n = 10$ ) (data not shown). (b) Flow cytometry analysis of Nur77 expression in DP thymocytes, before and 4 h after contact with antigen-loaded DCs, in the presence or absence of MK801 ( $100 \mu\text{M}$ ). The graphs are representative of three experiments. (c) Quantification of Nur77-expressing DP thymocytes before and 4 h after contact with HA-loaded DCs, in the presence or absence of MK801 ( $100 \mu\text{M}$ ). (d) Representative traces of the  $\text{Ca}^{2+}$  response in thymocytes in contact with HA-pulsed DCs. Thymocytes were preincubated with MK801 ( $100 \mu\text{M}$ ), NMDA ( $300 \mu\text{M}$ ) and D-serine ( $20 \mu\text{M}$ ) to block any NMDARs that would be present at the membrane before synapse formation. Thymocytes were then washed and added to HA-pulsed DCs in the absence or presence of the NMDAR antagonists MK801 ( $100 \mu\text{M}$ ). (e) Representative traces of the  $\text{Ca}^{2+}$  response in thymocytes in contact with HA-pulsed DCs MK801 ( $100 \mu\text{M}$ ) was applied after the beginning of  $\text{Ca}^{2+}$  response ( $t = 208$  s)

**Thymocyte–DC interaction induces NR1 and PSD-95 clustering at the contact zone.** Transient activation of NMDA channels at the synapse suggest that an important trafficking of these receptors could occur in thymocytes. The TCR signalosome includes PDZ domain-containing adaptors, increasingly thought to be involved in ISs.<sup>28</sup> Postsynaptic density (PSD)-95, accumulates in the active zones of neuronal synapses, forming so-called PSDs. It is the first-line signalling adaptor binding directly to the C-terminus of NMDAR subunits,<sup>29</sup> involved in stabilization and functional recruitment of NMDARs at the excitatory synapse.<sup>30</sup> Staining for NR1 and PSD-95 indicated that both were distributed over the entire resting thymocytes, but were colocalized in the contact zone in T-DC synapses (Figure 4a and Supplementary Figure S4). When thymocytes were stimulated with anti-CD3/CD28-coated beads in the absence of glutamate, PSD-95 was nonetheless colocalized with NR1 in the contact zone (Figure 4a), indicating that the relocalization of NMDAR and PSD-95 to the synapse depends on TCR stimulation. Interestingly, TCR stimulation using anti-CD3/CD28-coated beads, in the presence or absence of NMDA (or glutamate itself), did not recapitulate the effect of glutamate observed in a synaptic context. The  $\text{Ca}^{2+}$  signal was not sustained with a high-level plateau (Figures 4b and c), no significant apoptosis was induced

(data not shown) and no NMDA currents were recorded (data not shown), indicating that in addition to glutamate, one or several other signals provided by the DC, are necessary to activate NMDARs.

We conclude that intense trafficking of NMDAR may occur in thymocytes on contact with DCs. TCR triggering is sufficient to induce NR1 and PSD-95 clustering at the synapse, while the NMDAR is activated only in a complete synaptic context.

**DCs are capable of fast glutamate release.** As all the  $\text{Ca}^{2+}$  signalling experiments in T-DC contacts were performed in the absence of exogenous glutamate, we wondered which cell was the physiological source of glutamate. Immunostaining with a specific antibody to glutamate showed immunoreactivity mainly in DCs indicating that DC is the source of glutamate in T-DC synapses (Figure 5a). Moreover, DCs express the glutamate-specific vesicular glutamate transporters (VGLUT)1 and VGLUT2, which confer a glutamatergic phenotype to neurons<sup>31</sup> and VGLUT3 (Figure 5b and Supplementary Figure S5b). Vesicular structures of 100 nm size, with a characteristic electron-dense membrane were observed in DCs, opposite the contact zone and often located in a polarized cytoplasmic region-containing mitochondria (Figure 5c). Immunogold

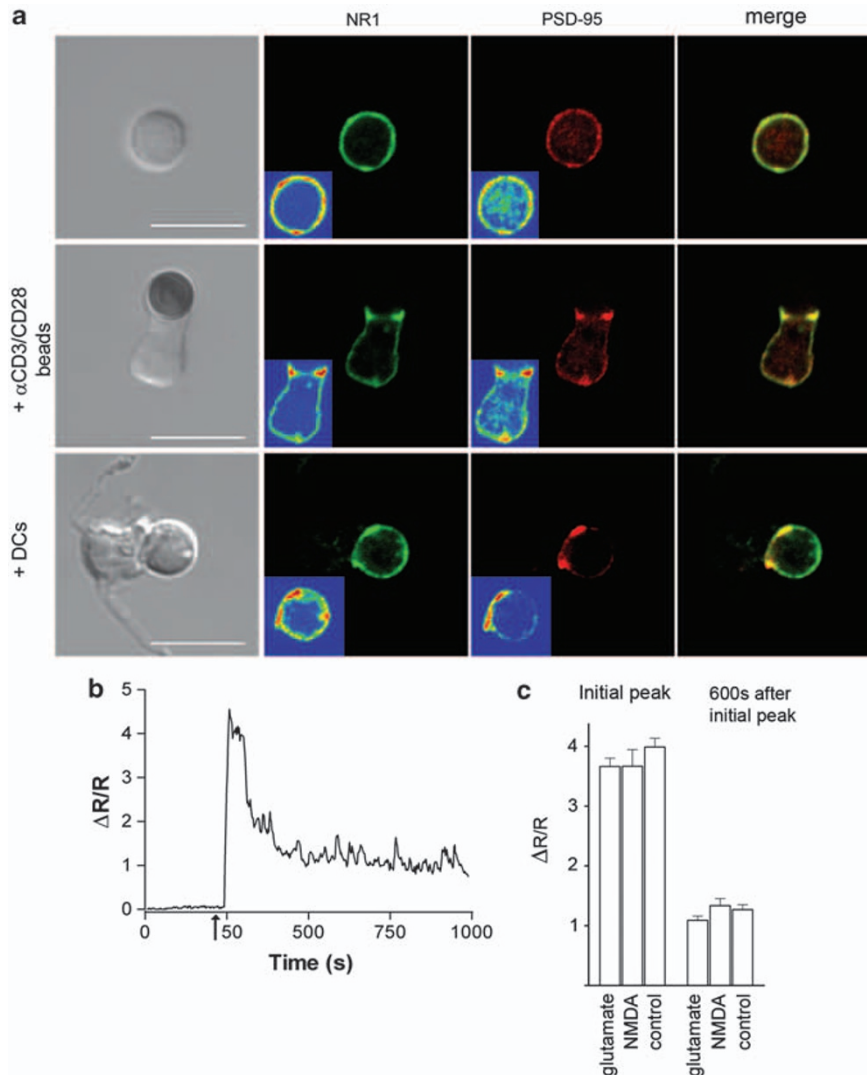


**Figure 4** TCR triggering is sufficient to induce NMDAR relocalization at the thymocyte-DC contact zone, whereas NMDAR can be activated only in a synaptic context. (a) Double labelling of PSD-95 (red) and NR1 (green) on isolated thymocytes, thymocytes in contact with anti-CD3/CD28-coated beads and thymocytes in contact with a DC. Merged pictures are shown in each case (yellow). Scale bars, 10  $\mu$ m. Profiles of distribution of fluorescence intensities and colocalization analysis of PSD-95 and NR1 are shown in Supplementary Figure S4. Controls consisted in mouse IgG2b isotype control for NR1 and purified rabbit IgG for PSD-95 (not shown). (b) Representative trace of  $Ca^{2+}$  response in thymocytes in contact with anti-CD3/CD28-coated beads. Arrow: contact. (c) Histogram of the mean  $Ca^{2+}$  amplitudes from 6 to 11 representative traces at the initial peak and at the plateau phase (600 s after the initial peak), in the absence or presence of glutamate (300  $\mu$ M) and NMDA (100  $\mu$ M)

labelling of VGLUT2 showed clusters of particles delineating discrete vesicles, opposite the contact zone in DCs (Figure 5d and Supplementary Figure S5d). Purified DCs express mRNAs encoding components involved in neurotransmitter exocytosis through SNARE complex formation (synaptophysin, Snap-23 and VAMP-2) or in the regulation of vesicle docking (Munc-18), as well as synaptotagmin-I (Supplementary Figures S5c and e), a  $Ca^{2+}$  sensor for glutamate release. VGLUT2 and synaptotagmin-I were co-expressed in the same vesicular structures (Figure 5e), suggesting the presence in DCs of a compartment competent for both glutamate accumulation and exocytosis. The question of glutamate production by immune cells was previously addressed, by measuring glutamate accumulation over 24 h in culture.<sup>18</sup> Instead, we focused on real-time

monitoring of glutamate release by freshly isolated DCs, using the L-glutamate dehydrogenase (GDH)-linked assay.<sup>32</sup> In the presence of external  $Ca^{2+}$ , ionomycin (Figure 5f) and SDF-1 $\alpha$  (a physiological stimulus in astrocytes)<sup>33,34</sup> (Figure 5g) triggered both  $[Ca^{2+}]_i$  increases and glutamate release in DCs with a similar time course.

We conclude that DCs show features required for regulated glutamate exocytosis and are capable of fast glutamate release in a  $Ca^{2+}$ -dependent manner.

## Discussion

In previous studies, GluRs were potentially involved in immune regulation,<sup>3</sup> T cells were thought to be exposed to glutamate in the CNS, in the bloodstream or in certain

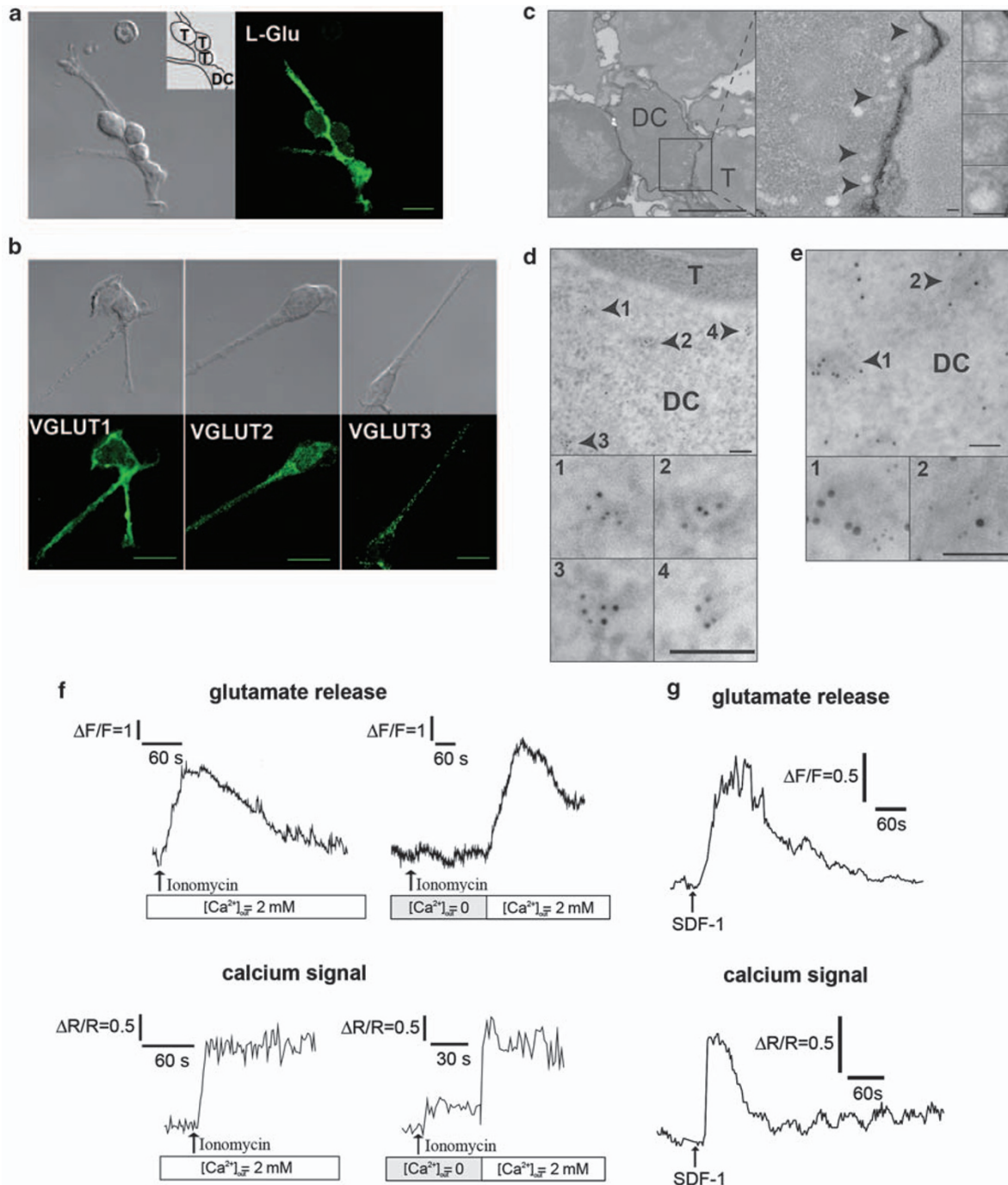


**Figure 5** DCs may be the physiological source of glutamate in thymocyte-DC synapses. (a) Confocal immunofluorescence image of glutamate labelling in a DC in contact with three thymocytes (right). Corresponding Nomarski image (left), with an inset indicating the cell contours. Scale bar, 10  $\mu\text{m}$ . (b) Immunofluorescence analysis of VGLUT1, VGLUT2 and VGLUT3 in DCs (bottom row), with the corresponding Nomarski images (top row). Scale bar, 10  $\mu\text{m}$ . Typical punctate fluorescent staining of VGLUT2 and VGLUT3, was observed in DCs (Supplementary Figure S5b). (c) Morphological electron micrograph of thymocyte-DC conjugates showing a group of vesicle structures at the cell-cell interface. Original image (left, scale bar, 2  $\mu\text{m}$ ). Magnification of the synapse (middle, scale bar, 100 nm) and of the vesicles (right, scale bar, 100 nm). Arrows: individual vesicles in the DC. (d) Immunogold staining of VGLUT2 in the T cell-DC contact zone. Top: low magnification with vesicles in the DC indicated by arrows. Bottom: higher magnification. Scale bar, 100 nm. (e) Immunogold colocalization of VGLUT2 (5 nm) and synaptotagmin I (10 nm) on the same vesicular structures (arrows). Top: individual vesicles indicated by arrows (scale bar, 2  $\mu\text{m}$ ). Bottom: magnifications (scale bars, 100 nm). Control staining is shown in Supplementary Figure S5d (f) Typical traces of glutamate release (upper panels) from DCs stimulated with ionomycin (1  $\mu\text{M}$ ), monitored in continuous culture, by recording NADH fluorescence emission. Horizontal scale: time in seconds. Vertical scale: arbitrary units. The amounts of glutamate released represented 40% of the fluorescence increase induced by 10  $\mu\text{M}$  glutamate. Lower panels:  $\text{Ca}^{2+}$  signals induced by ionomycin in the presence or absence of extracellular  $\text{Ca}^{2+}$  in Fura-2-loaded DCs. (g) Typical traces of glutamate release (upper panel) from DCs stimulated with SDF-1 $\alpha$  (100 nM), monitored as in (f). Bottom panel:  $\text{Ca}^{2+}$  signal induced by SDF-1 $\alpha$  in Fura-2-loaded DCs, in the presence of extracellular  $\text{Ca}^{2+}$ .



peripheral organs<sup>7</sup> and monocyte-derived DCs have been pointed out as a source of slow glutamate release accumulating in T-DC long-term cocultures.<sup>18</sup> As T cells communicate through ISs, which are structurally similar to neuronal synapses,<sup>16</sup> several questions are left unanswered. Does the IS use glutamate signalling? Is that signalling linked to  $\text{Ca}^{2+}$  signals governing T-cell fate? How important is synapse structure in glutamatergic communication between T cells and DCs? To what extent are immunological and neuronal synapses functionally similar?

**The NMDAR, a source of  $\text{Ca}^{2+}$  entry in T-cell signalling at the IS.** Until recently, most of the studies examining  $\text{Ca}^{2+}$  entries in T cells were not carried out on T cells contacting APCs. Thymocytes responded to DC contact with an immediate  $\text{Ca}^{2+}$  signal, with a sustained plateau sensitive to NMDAR blockers. Our data suggest that this sustained  $\text{Ca}^{2+}$  signal is probably not due to a sustained activity of the NMDAR. Similarly to the mechanisms involved in synaptic plasticity (LTD and LTP)<sup>35</sup> there might be a transient activation of NMDARs, which could act as a trigger of a sustained  $\text{Ca}^{2+}$  response carried by other effectors. However, no detectable NMDAR signal was observed in resting thymocytes and in thymocytes stimulated with anti-CD3/CD28-coated beads (i.e., not engaged in a full synapse with DCs). It is physiologically relevant that the contact with DC may be necessary to activate NMDARs. Our observation that sustained  $\text{Ca}^{2+}$  signalling and apoptosis occurred only in the context of IS and not in solitary thymocytes is in line with the need for a tight control of T-cell activation by antigen-specific contact with DC, to ensure proper thymic negative selection. Indeed, the IS is the physiological structure dedicated to communication in the immune system and represents a logical strategy to provide protection against permanent exposure of thymocytes to glutamate. Such a strategy could also make sense in activation of peripheral T cells, which are exposed to substantial glutamate concentration in serum. The sustained, high-level  $\text{Ca}^{2+}$  plateau observed in this study was characteristic of thymocytes and correlated with antigen-dependent induction of apoptosis. It was not observed in naïve peripheral  $\text{CD4}^+$  splenic T cells that showed glutamate signalling-dependent proliferation (PA and SC-K unpublished data) but no apoptosis. The correlation between T-cell fate and the shape of the  $\text{Ca}^{2+}$  signal suggests that the elevated plateau phase is intimately linked to thymocyte apoptosis. This opens new challenges to identify the switches controlling pro-survival *versus* pro-apoptosis outcome of NMDAR stimulation.

**DC, a site of glutamate mobilization for exocytosis signalling.** A recent study in T cells cocultured with monocyte-derived DCs pulsed with a superantigen, showed glutamate production in the milieu, detectable from day 1 (in the  $5\ \mu\text{M}$  range) and accumulating in the coculture with time. This glutamate production involved a slow release mechanism, mediated by the cystine/glutamate antiporter.<sup>18</sup> In this study, we showed a rapid and substantial release of glutamate by DCs, consistent with previous reports of synaptic polarization and  $\text{Ca}^{2+}$ -regulated release of pre-assembled

vesicular cytokine stores for DCs.<sup>36</sup> We used several approaches to suggest that DCs are competent for both glutamate accumulation and release. (1) Immunofluorescence showed strong punctate staining for glutamate and VGLUT vesicular transporters, and staining for the  $\text{Ca}^{2+}$  sensor synaptotagmin-I and for VAMP-2, a SNARE component of the vesicular machinery for exocytosis. (2) Electron microscopy showed vesicle-like structures in the T-DC contact zones. (3) Double immunogold staining suggested that DCs are competent for both glutamate accumulation mediated by VGLUT and glutamate release through a  $\text{Ca}^{2+}$ - and SNARE-dependent mechanism. (4) An enzymatic-linked assay showed ionomycin and SDF-1 $\alpha$ -induced L-glutamate release by DCs. It remains to define the precise SNARE-dependent mechanism of exocytosis, using specific drugs or toxins, and to determine the type of  $\text{Ca}^{2+}$  entry involved in exocytosis signalling; mechanisms similar to those reported for astrocytes might be expected.<sup>33</sup> In our hands, riluzole and bafilomycin inhibited the  $\text{Ca}^{2+}$  signal and caspase-3 induction in thymocytes contacting DCs (PA and SC-K unpublished data). However, this approach is not entirely appropriate as exocytosis of chemokines might be also affected. Indeed, we have shown that SDF-1 $\alpha$ , a physiological stimulus-mobilizing intracellular  $\text{Ca}^{2+}$ ,<sup>34</sup> triggers the release of glutamate from DCs. How SDF-1 operates in the minimal system of T-DC synapses for glutamate release remains to be determined.  $\text{Ca}^{2+}$  transients in DCs interacting with T cells may be involved in triggering glutamate exocytosis, but they have rarely been observed here and in human DCs,<sup>34</sup> suggesting that local  $\text{Ca}^{2+}$  fluxes in DCs might be involved in glutamate release. As thymic epithelial cells, did not release measurable glutamate in real-time (PA, TC and SC-K, unpublished data), DCs may be specialized for rapid glutamate delivery to T cells. Glutamate should be considered an 'immunotransmitter' as suggested for cytokines and chemokines.<sup>37</sup>

**PSD-95, a signalling adaptor indicative of the glutamatergic phenotype of the IS.** In neuronal synapses, PSDs, which contain an intricate network of scaffolding PDZ-domain proteins, are thought to participate in synapse genesis and to organize  $\text{Ca}^{2+}$  sources, sensors and effectors, and a number of signalling proteins.<sup>30</sup> Several studies showed a role for PDZ-domain proteins such as CARMA1<sup>38</sup> and hDlg/Dlg1/SAP97<sup>28</sup> in T-cell activation and TCR activation-induced synapse assembly, respectively. Our findings add to the current knowledge the possibility of PSD-95-mediated connections between NMDARs and TCRs. Although the role of GluRs in T-DC communication was not entirely unexpected, we were surprised to find that TCR triggering alone was sufficient to promote the clustering of both NMDAR and PSD-95 in the contact zone. We suggest that TCR signalling triggers the modelling of the nascent IS into a functionally competent synapse for glutamate signalling. Hence, our data indicated that NMDAR can be activated only in a synaptic context. An additional signal from the DC may be needed to activate NMDARs. We suggest that the IS may provide a functional platform for coupling detection of TCR ligation and NMDAR activation with subsequent focal NMDAR signalling. PSD-95 may well be a primary adaptor, connecting TCR and NMDAR



signalling. A challenge will be to understand the precise molecular mechanism of the interconnection between TCR and NMDAR signalling. Furthermore, a transient activation of NMDARs at the synapse would suggest an important trafficking of these receptors in thymocytes. Although our data indicate that PSD95 might be involved, the mechanism of NMDAR exocytosis at the synapse as showed in neurones<sup>35</sup> remains to be solved.

In conclusion, for years, glutamate signalling was thought to take place primarily in the CNS; it is now known to control key peripheral physiological functions, such as insulin secretion, keratinocyte differentiation, and remodelling of bone mass. Accordingly, therapeutic applications are being developed for diabetes, psoriasis, and osteoporosis.<sup>2</sup> Our findings suggest an additional site of peripheral glutamate signalling and possible involvement of NMDARs in a major physiological function of the thymus: the negative selection. There is still a long road to solve the complexity of the cooperation of different GluRs in T-DC synapses. Understanding the precise role of glutamate signalling in determining T-cell fate by modulating the proliferation/differentiation balance, the effector/regulatory and effector/memory transitions, might reflect on the physiology of the adaptive immune response. Our findings together with previous data<sup>3</sup> raise potential applications for drug-mediated immunomodulation through interactions with L-glutamate signalling.

#### Materials and Methods

**Mice.** The generation and genotyping of HNT-TCR transgenic mice specific for the HA 126–138 (HNTGVTAACSHE) peptide presented by MHC class II I-A<sup>d</sup> have been described elsewhere.<sup>24</sup> All animals had a B10.D2 (H2<sup>d</sup>) genetic background and were used at the age of 6–10 weeks. All animal experiments conformed to European Community guidelines of animal protection and local legal and ethical requirements. All experiments were approved by local authorities and direction des Services Veterinaires des Hauts-De-Seine (authorization for animal experimentation to SC-K, No. 92–131). T cells and DCs were isolated, purified and cocultured using standard methods as described in Supplementary online Materials and Methods.

**Antibodies and reagents.** All antibodies were proved to be specific and are widely used in the neuronal system. Antibodies against NR2A and NR2B were purchased from Upstate Biotechnology (Millipore SAS, Molsheim, France). Antibodies against NR1 (M68), VGLUT1, VGLUT2 and VGLUT3 used in flow cytometry or confocal microscopy were from Synaptic Systems (Goettingen, Germany). Anti-NR1 antibody M68, widely used in neurones, recognized a band at the expected molecular weight (116 KD) in western blotting experiments of rat brain microsomal preparations and of thymocytes extracts immunoprecipitated by anti-PSD-95 (data not shown). Biotinylated anti-CD3 (145–2C11) and anti-CD28 (37.51) were from Pharmingen (BD Biosciences, Le Pont de Claix, France). Antibodies against PSD-95 and glutamate were from Zymed (San Francisco, CA, USA) and Sigma-Aldrich (Lyon, France), respectively. All inhibitors and antagonists specific for GluRs were from Tocris (Bristol, UK).

**DNA chip analysis of the GluR repertoire.** DNA chip analysis was performed on Neurotrans NT280M oligochips from GeneScore ([www.genescore.fr](http://www.genescore.fr)), registered on GEO (Gene Expression Omnibus) (No GPL4746), already used for studies in the CNS and containing oligonucleotides for 280 genes involved in neurotransmission (two oligonucleotides for each gene).<sup>39</sup> Modifications are available in Supplementary online Materials and Methods.

**Single-cell Ca<sup>2+</sup> video imaging.** Single-cell Ca<sup>2+</sup> video imaging on T-DC conjugates was carried out using a modified version of a previously described method.<sup>40</sup> Purified DCs were plated on glass delta T culture dishes (Bioprotechs, Butler, PA, USA) coated with polylysine and maintained at 37 °C in recording solution (mammalian saline: 116 mM NaCl, 5.6 mM KCl, 1.2 mM MgCl<sub>2</sub>, 2 mM CaCl<sub>2</sub>, 5 mM NaHCO<sub>3</sub>, 1 mM NaH<sub>2</sub>PO<sub>4</sub>, 20 mM HEPES, pH 7.3, supplemented with

2 g/l glucose). Thymocytes or CD4<sup>+</sup> T cells were loaded for 30 min with 4 μM Fura-2/AM (Molecular Probes, Invitrogen, Cergy Pontoise, France) by incubation for 30 min at 37 °C in culture medium. When indicated T cells were preincubated for 10 min with the NMDAR antagonists and then dispensed on top of the DCs maintained at 37 °C using a temperature-controlled dish, which was fixed above a warmed epifluorescence 40 × oil objective (Bioprotechs, Farmingdale, NY, USA) and a PTR 200 perfusion temperature regulator (ALA Scientific Instruments, Farmingdale, NY, USA). Successive fluorescence and DIC images were recorded for 20 min. Light for excitation was supplied by a high pressure 100 W xenon arc lamp and the 340 and 380 nm wavelengths were selected with a monochromator (Cairn Research Ltd, Faversham Kent, UK). Fluorescence images were collected with a Sencicam QE CCD camera (PCO Computer Optics GmbH, Kelheim, Germany), digitized, and integrated in real time by an image processor (Metafluor, Molecular Devices, Downingtown, PA, USA). The light transmission images were taken every 6 s, alternating with the fluorescent images. The fluorescent signals were analyzed offline, using an image processor (Metamorph, Molecular Devices) to account for cell movements during the 20-min recordings. Background fluorescence was subtracted from the corresponding fluorescent images. To allow comparison between different labs, results are expressed as ( $\Delta R/R$ ), where R is the ratio (R) between fluorescence signals at 340 and 380 nm obtained before the addition of any agent, and  $\Delta R$  the difference between the ratios measured during a response and R. For single cell Ca<sup>2+</sup> video imaging in isolated thymocytes and DCs, a modification of this protocol was used and is provided in Supplementary online Materials and Methods.

**Extracellular glutamate imaging.** We used the L-GDH-linked assay, a fluorescence-based assay allowing dynamic quantification of glutamate release in non-excitabile cells, to monitor rapid glutamate release from DCs.<sup>32</sup> Purified DCs ( $5 \times 10^5$ ) were incubated for 20 min on glass coverslips treated with polylysine, to allow adhesion. DCs were washed and bathed in the recording solution (mammalian saline as above, supplemented with NAD (1 mM), and L-GDH at 50 IU/ml (Sigma-Aldrich)). Glutamate released from the cells was immediately oxidized to  $\alpha$ -ketoglutarate by GDH, with the formation of NADH and fluorescence emission at 450 nm. Controls without L-GDH indicated that detectable levels of NADH are not produced by DCs, either spontaneously or after induction by ionomycin. Agents were added directly to the culture dish.

**Flow cytometry and confocal microscopy.** Flow cytometry (four colour flow cytometry, activated caspase-3 detection and Ca<sup>2+</sup> flux studies) and confocal microscopy on T-DC conjugates were performed using standard procedures as described in Supplementary online Materials and Methods. The controls consisted of mouse isotype controls (as control for the monoclonal M68 anti-NR1, anti-Nur77 and anti-synaptotagmine antibodies), and purified rabbit IgG as control for anti-NR2A, NR2B, GluR2/3, PSD-95, KA2, glutamate, VGLUT antibodies. The same settings and exposure time were used for image acquisition by confocal microscopy of the specific staining and the controls.

**Electron microscopy.** Morphological analysis and post-embedding immunocytochemistry and immunogold labelling of T-DC conjugates was performed using classical techniques as described in Supplementary online Materials and Methods. Mouse isotype controls and purified rabbit IgG were used as controls for immunogold staining, with the same exposure time and magnification as specific staining.

**Statistical analysis.** Data are expressed as means  $\pm$  S.E.M. Statistical significance was assessed by the non-parametric Mann–Whitney test, using Prism, version 5.0, software (GraphPad Software, San Diego, CA, USA). The significance level was set at  $P = 0.05$ . The Kolmogorov–Smirnov test (Cellquest Software, BD Biosciences) was used to compare FACS profiles.

#### Conflict of Interest

The authors declare no conflict of interest.

**Acknowledgements.** We thank A Trautmann and B Malissen for helpful discussions and critical reading of the paper. We thank JF Renaud and A Lombet for continuous support and N Kerlero de Rosbo for reading the paper. We thank B Lucas for helpful discussions. We thank C Rucker-Martin and V Nicolas for advice

and assistance on confocal microscopy, L Dauphinot for expertise in PCR, D Jaillard for excellent assistance with electron microscopy, JP Mauger and S Wick for access to the animal facility. This work was supported by grants from *Association de la Recherche contre le Cancer* (to SC-K and to TC), *Fondation de France* (to SC-K), *Bonus Qualité Recherche de l'Université Paris-Sud* (to OM and SC-K), *Centre National de la Recherche Scientifique, Conseil Régional Ile de France (Sesame)* and *Association Marie Lannelongue*. PA was supported as a PhD candidate by a studentship from the *Ministère de l'Éducation nationale, de la Recherche et de la Technologie*. GLC and SP are supported by the Medical Research Council. GLC is a Royal Society-Wolfson Merit Award Holder.

- Nedergaard M, Takano T, Hansen AJ. Beyond the role of glutamate as a neurotransmitter. *Nat Rev Neurosci* 2002; **3**: 748–755.
- Skerry TM, Genever PG. Glutamate signalling in non-neuronal tissues. *Trends Pharmacol Sci* 2001; **22**: 174–181.
- Pacheco R, Gallart T, Lluís C, Franco R. Role of glutamate on T-cell mediated immunity. *J Neuroimmunol* 2007; **185**: 9–19.
- Pacheco R, Ciruela F, Casado V, Mallol J, Gallart T, Lluís C *et al*. Group I metabotropic glutamate receptors mediate a dual role of glutamate in T cell activation. *J Biol Chem* 2004; **279**: 33352–33358.
- Chiocchetti A, Miglio G, Mesturini R, Varsaldi F, Mocellini M, Orilieri E *et al*. Group I mGlu receptor stimulation inhibits activation-induced cell death of human T lymphocytes. *Br J Pharmacol* 2006; **148**: 760–768.
- Boldyrev AA, Carpenter DO, Johnson P. Emerging evidence for a similar role of glutamate receptors in the nervous and immune systems. *J Neurochem* 2005; **95**: 913–918.
- Ganor Y, Besser M, Ben-Zakay N, Unger T, Levite M. Human T cells express a functional ionotropic glutamate receptor GluR3, and glutamate by itself triggers integrin-mediated adhesion to laminin and fibronectin and chemotactic migration. *J Immunol* 2003; **170**: 4362–4372.
- Lombardi G, Dianzani C, Miglio G, Canonico PL, Fantozzi R. Characterization of ionotropic glutamate receptors in human lymphocytes. *Br J Pharmacol* 2001; **133**: 936–944.
- Miglio G, Varsaldi F, Lombardi G. Human T lymphocytes express N-methyl-D-aspartate receptors functionally active in controlling T cell activation. *Biochem Biophys Res Commun* 2005; **338**: 1875–1883.
- Lewis RS. Calcium signaling mechanisms in T lymphocytes. *Annu Rev Immunol* 2001; **19**: 497–521.
- Vig M, Peinelt C, Beck A, Koomoa DL, Rabah D, Koblan-Huberson M *et al*. CRACM1 is a plasma membrane protein essential for store-operated Ca<sup>2+</sup> entry. *Science* 2006; **312**: 1220–1223.
- Kotturi MF, Hunt SV, Jefferies WA. Roles of CRAC and Cav-like channels in T cells: more than one gatekeeper? *Trends Pharmacol Sci* 2006; **27**: 360–367.
- Norcross MA. A synaptic basis for T-lymphocyte activation. *Ann Immunol (Paris)* 1984; **135D**: 113–134.
- Huse M, Lillemeier BF, Kuhns MS, Chen DS, Davis MM. T cells use two directionally distinct pathways for cytokine secretion. *Nat Immunol* 2006; **7**: 247–255.
- Brossard C, Feuillet V, Schmitt A, Randriamampita C, Romao M, Raposo G *et al*. Multifocal structure of the T cell – dendritic cell synapse. *Eur J Immunol* 2005; **35**: 1741–1753.
- Dustin ML, Colman DR. Neural and immunological synaptic relations. *Science* 2002; **298**: 785–789.
- Steinman L. Elaborate interactions between the immune and nervous systems. *Nat Immunol* 2004; **5**: 575–581.
- Pacheco R, Oliva H, Martínez-Navio JM, Climent N, Ciruela F, Gatell JM *et al*. Glutamate released by dendritic cells as a novel modulator of T cell activation. *J Immunol* 2006; **177**: 6695–6704.
- Arundine M, Tymianski M. Molecular mechanisms of calcium-dependent neurodegeneration in excitotoxicity. *Cell Calcium* 2003; **34**: 325–337.
- Palmer E. Negative selection—clearing out the bad apples from the T-cell repertoire. *Nat Rev Immunol* 2003; **3**: 383–391.
- Mayer ML, Armstrong N. Structure and function of glutamate receptor ion channels. *Annu Rev Physiol* 2004; **66**: 161–181.
- Storto M, de Grazia U, Battaglia G, Felli MP, Maroder M, Gulino A *et al*. Expression of metabotropic glutamate receptors in murine thymocytes and thymic stromal cells. *J Neuroimmunol* 2000; **109**: 112–120.
- Collingridge GL, Olsen RW, Peters J, Spedding M. A nomenclature for ligand-gated ion channels. *Neuropharmacology* 2009; **56**: 2–5.
- Liblau RS, Tisch R, Shokat K, Yang X, Dumont N, Goodnow CC *et al*. Intravenous injection of soluble antigen induces thymic and peripheral T-cells apoptosis. *Proc Natl Acad Sci U S A* 1996; **93**: 3031–3036.
- Woronicz JD, Calnan B, Ngo V, Winoto A. Requirement for the orphan steroid receptor Nur77 in apoptosis of T-cell hybridomas. *Nature* 1994; **367**: 277–281.
- Cho HJ, Edmondson SG, Miller AD, Sellars M, Alexander ST, Somersan S *et al*. Cutting edge: identification of the targets of clonal deletion in an unmanipulated thymus. *J Immunol* 2003; **170**: 10–13.
- Merkenschlager M, Graf D, Lovatt M, Bommhardt U, Zamoyska R, Fisher AG. How many thymocytes audition for selection? *J Exp Med* 1997; **186**: 1149–1158.
- Round JL, Tomassian T, Zhang M, Patel V, Schoenberger SP, Miceli MC. Dlg1 coordinates actin polymerization, synaptic T cell receptor and lipid raft aggregation, and effector function in T cells. *J Exp Med* 2005; **201**: 419–430.
- Kornau HC, Schenker LT, Kennedy MB, Seeburg PH. Domain interaction between NMDA receptor subunits and the postsynaptic density protein PSD-95. *Science* 1995; **269**: 1737–1740.
- Kim E, Sheng M. PDZ domain proteins of synapses. *Nat Rev Neurosci* 2004; **5**: 771–781.
- Takamori S, Rhee JS, Rosenmund C, Jahn R. Identification of a vesicular glutamate transporter that defines a glutamatergic phenotype in neurons. *Nature* 2000; **407**: 189–194.
- Innocenti B, Parpura V, Haydon PG. Imaging extracellular waves of glutamate during calcium signaling in cultured astrocytes. *J Neurosci* 2000; **20**: 1800–1808.
- Bezzi P, Domercq M, Brambilla L, Galli R, Schols D, De Clercq E *et al*. CXCR4-activated astrocyte glutamate release via TNF $\alpha$ : amplification by microglia triggers neurotoxicity. *Nat Neurosci* 2001; **4**: 702–710.
- Montes M, McIlroy D, Hosmalin A, Trautmann A. Calcium responses elicited in human T cells and dendritic cells by cell-cell interaction and soluble ligands. *Int Immunol* 1999; **11**: 561–568.
- Collingridge GL, Isaac JT, Wang YT. Receptor trafficking and synaptic plasticity. *Nat Rev Neurosci* 2004; **5**: 952–962.
- Borg C, Jalil A, Laderach D, Maruyama K, Wakasugi H, Charrier S *et al*. NK cell activation by dendritic cells (DCs) requires the formation of a synapse leading to IL-12 polarization in DCs. *Blood* 2004; **104**: 3267–3275.
- Trautmann A. Chemokines as immunotransmitters? *Nat Immunol* 2005; **6**: 427–428.
- Jun JE, Wilson LE, Vinuesa CG, Lesage S, Blery M, Miosge LA *et al*. Identifying the MAGUK protein Carma-1 as a central regulator of humoral immune responses and atopy by genome-wide mouse mutagenesis. *Immunity* 2003; **18**: 751–762.
- Potier MC, Gibelin N, Cauli B, Le Bourdelles B, Lambalez B, Golfier G *et al*. Development of microarrays to study gene expression in tissue and single cells: analysis of neural transmission. In: Geschwind DH, Gregg JP, (Eds) *Microarrays for the Neurosciences: An Essential Guide*. MIT Press: Cambridge, 2002. pp 237–254.
- Delon J, Bercovici N, Raposo G, Liblau R, Trautmann A. Antigen-dependent and -independent Ca<sup>2+</sup> responses triggered in T cells by dendritic cells compared with B cells. *J Exp Med* 1998; **188**: 1473–1484.

Supplementary Information accompanies the paper on Cell Death and Differentiation website (<http://www.nature.com/cdd>)